International Journal of Minerals, Metallurgy and Materials
Volume 27, Number 8, August 2020, Page 1123
https://doi.org/10.1007/s12613-019-1949-8

Evaluation on elevated-temperature stability of modified 718-type alloys with varied phase configurations

Zhan Qiao[1)], *Chong Li*[1)], *Hong-jun Zhang*[2)], *Hong-yan Liang*[1)], *Yong-chang Liu*[1)], *and Yong Zhang*[3)]

1) State Key Lab of Hydraulic Engineering Simulation and Safety, School of Materials Science & Engineering, Tianjin University, Tianjin 300354, China
2) Key Laboratory of the Ministry of Education for Modern Metallurgy Technology, North China University of Science and Technology, Tangshan 063210, China
3) Science and Technology on Advanced High Temperature Structural Materials Laboratory, AEEC Beijing Institute of Aeronautical Materials, Beijing 100095, China
(Received: 17 October 2019; revised: 1 December 2019; accepted: 11 December 2019)

Abstract: Inconel 718 is a Ni–Fe-based superalloy widely used in aerospace engines because of its excellent mechanical properties. However, the inferior stability of the γ″ phase limits the application of Inconel 718, which coarsens rapidly at temperatures greater than 650°C. Further improving the temperature tolerance of Inconel 718 requires optimization of the phase configuration via modification of the alloy's chemical composition. Given the aforementioned objective, this work was conducted to study the precipitation behavior and thermal stability of the strengthening phases with various structures in modified Inconel 718 alloys by tailoring the Al/Ti ratio. With increasing Al/Ti ratio, three particle configurations were formed: γ′/γ″ composite, isolated γ′, and γ′/γ″/γ′ composite particles. The results of aging tests demonstrate that the isolated γ′ and the γ′/γ″/γ′ composite structure exhibited better thermal stability at temperature as high as 800°C. The isolated γ′ exhibited a reduced coarsening rate compared with the γ′/γ″/γ′ composite particles because the isolated γ′ phase was rich in Al, Ti, and Nb. However, the γ′/γ″ composite particles coarsened and decomposed rapidly during aging at temperatures greater than 700°C because of the lower stability resulting from the larger number of γ″ particles. The obtained results provide necessary data for the compositional optimization of novel 718-type alloys.

Keywords: Inconel 718; structure; thermal stability; interface

1. Introduction

Inconel 718 is one of the most widely used Ni–Fe-based superalloys in aerospace engines because of its excellent corrosion resistance, high strength, and good weldability. Its superior high temperature mechanical strength is attributed to the major γ″-Ni_3Nb precipitates ($D0_{22}$ structure) with a lens-like shape and few γ′-Ni_3Al precipitates ($L1_2$ structure) with an ellipsoidal shape[1–3]. However, the metastability of the γ″ phase makes it transform into a stable orthorhombic δ-Ni_3Nb phase during long-term exposure at temperatures greater than 650°C [4–6]. The formation of the δ-Ni_3Nb phase results in deterioration of the properties of the alloy, which affects the future application of this material in advanced turbine disks [7–9]. With the development of the aviation industry, stricter requirements are being imposed on turbine engines [10], necessitating the development of wrought superalloys with enhanced stability at high temperatures [11].

Researchers [12–17] have previously attempted to improve the structural stability of Inconel 718 and to design novel modified 718 alloys for use at temperatures greater than 650°C via composition modifications. In the case of Inconel 718 alloy, Al is critical to the formation of the γ′ phase and can increase the γ′ solvus and fraction; Ti plays an important role in the formation of the γ″ phase. By comparison, Nb exhibits no obvious ability to promote the precipitation of γ′; however, Nb can dissolve into the γ′ lattice and improve the thermal stability of the γ′ phase [18]. Previous works [15–17,19–21] have attempted to regulate the constituents of the γ″ and γ′ phases by adjusting the relative Al, Ti, and Nb contents. Enhancing the Al + Ti content and Al/Ti ratio can not only change the γ′ solvus and proportion of γ″ and γ′ phases [18] but also inhibit the formation of δ and η phases [21–22]. More important, the morphology of strengthening precipitates appears to change with compositional modifica-

Corresponding authors: Chong Li E-mail: lichongme@tju.edu.cn; Hong-jun Zhang E-mail: zhanghongjunzg@163.com; Yong-chang E-mail: Liu licmtju@163.com

tions [23–24]. Cozar and Pineau [25] first discovered γ″/γ′ particles with a compact morphology by changing the composition of Inconel 718 superalloy such that cubic γ′ precipitated in the middle, whereas γ″ formed at the six γ′/γ interfaces. Similar works [26–27] have confirmed that modified Inconel 718 superalloys with compact morphology exhibit enhanced thermal stability because the compact precipitates grow more slowly. For other cases, γ″ and γ′ precipitates can form γ′/γ″ and sandwich-like γ″/γ′/γ″ coprecipitates [25]. However, these coprecipitates can also suffer rapid coarsening at temperatures greater than 650°C because of the existence of the γ″ phase; this problem remains to be solved.

Because its lattice structure is identical to that of the γ matrix, the γ′ phase exists in a coherent state, and is more thermally stable than the γ″ phase [28–29]. One of the methods is to form another sandwich-like structure of γ′/γ″/γ′, in which the growth and coarsening of the intermediate γ″ phase are suppressed by γ′ phase on the both sides. The other idea is to convert the γ″ strengthening alloy into a predominantly γ′ strengthening alloy. These two structures are expected to achieve higher thermal stability of the developed Inconel 718 superalloys.

In the present paper, to evaluate the thermal stability of precipitates with various morphologies, three precipitates—γ′/γ″ composite, isolated γ′, and γ′/γ″/γ′ composite precipitates—were obtained by modifying the Al/Ti ratio of Inconel 718 alloy; their precipitation behaviors and thermal stabilities were compared via aging treatments. On the basis of the experimental results, the dependence of the precipitation mechanisms on the Al/Ti ratio was discussed and the relationships between morphology, chemical composition, and thermal stability of the γ″ and γ′ phases were investigated.

2. Experimental

The experimental materials were processed through the powder metallurgy spark plasma sintering (SPS) route. To obtain samples with different Al/Ti ratios, Al (3N5 purity, ~48 μm), Ti (4N purity, ~ 48 μm), and conventional 718 alloy powder (~48 μm) were mixed in different weight ratios and stainless steel balls were put into the stainless steel container for grinding. The weight ratio between the balls and mixed powders was chosen as 10:1. All of the aforementioned operations were performed under an argon atmosphere. A planetary ball mill was used for mechanical alloying. After being ground for 5 h, the powders were collected, pressed into a cylindrical shape in a graphite die, and then sintered under vacuum in an SPS machine. The temperature was increased to 800°C at a rate of 100°C/min and then to higher temperatures at a rate of 50°C/min. When the temperature was ramped to 1100°C, the mixed powders were maintained at a pressure of 40 MPa for 10 min. The cylindrical specimens 20 mm in height and 20 mm in diameter were obtained by SPS sintering; their chemical compositions are shown in Table 1. After SPS, samples were removed for homogenization at 1190°C for 24 h and then cooled to room temperature in air. A heat treatment procedure for conventional 718 alloy was adopted for all of the modified alloys as follows: solution treatment (samples were kept at 980°C for 1 h and then cooled to room temperature in air) + double aging (samples were kept at 720°C for 8 h, then cooled to 620°C in the furnace, and kept at 620°C for 8 h next, then cooled to room temperature in air). To investigate the thermal stability of the precipitates with different structures, the specimens were subjected to an aging treatment at 700 or 800°C for different periods.

Table 1. Chemical compositions of the explored modified Inconel 718 alloys processed by SPS wt%

Specimen	Ni	Cr	Co	Mo	Nb	Al	Ti	Fe
Al/Ti ratio ≈ 1:1	50–55	19.72	0.09	2.92	4.97	0.78	0.78	Bal.
Al/Ti ratio ≈ 2:1	50–55	19.72	0.09	2.91	4.97	1.56	0.80	Bal.
Al/Ti ratio ≈ 3:1	50–55	19.70	0.09	2.91	4.96	2.32	0.82	Bal.

To characterize the microstructure of the modified Inconel 718 alloys after heat treatment, SiC abrasive papers were used to polish the surfaces of the specimens; the surfaces of the specimens were then treated by chemical etching. The composition of the adopted etchant was 5 g $CuCl_2$ + 100 mL HCl + 100 mL CH_3CH_2OH, and the etching time was 5 min. The morphologies of precipitates were observed by scanning electron microscopy (SEM), and the magnified morphologies and chemical composition of the local phase were characterized by energy-dispersive spectroscopy (EDS). The magnified morphologies were further observed by transmission electron microscopy (TEM). For the preparation of the TEM specimens, 0.3 mm-thick sheets were cut from the heat-treated superalloy samples; the foils were ground to a thickness of 50 mm using SiC abrasive paper, and electro polishing was performed using an electrolytic solution (5vol% $HClO_4$ + 95vol% CH_3CH_2OH). All specimens were tilted toward the {001} zone axis for detection of the γ″ and γ′ precipitates.

3. Results and discussion

3.1. Thermal stability of precipitates with varied structures

3.1.1. γ′/γ″ coprecipitates (Al/Ti ratio ≈ 1:1, wt%)

After the standard solution + two-stage aging heat treat-

ment, intragranular coprecipitation was observed in the modified alloy with an Al/Ti ratio of 1:1 (wt%), as illustrated in the dark-field TEM image in Fig. 1(a). The average particle size was calculated to be approximately 20 nm. The typical diffraction pattern along the $[001]_\gamma$ direction (Fig. 1(b)) clearly indicates the bimodal super lattice diffraction patterns of the γ″ and γ′ phases on the γ matrix; thus, these coprecipitates can be described as spherical γ′ particles covered by one or two γ″ particles on its surfaces.

Afterwards, the samples were aged at 700°C for 100 h to explore the evolution of the coprecipitates; the corresponding SEM morphology is shown in Fig. 2(a). The intragranular particles exhibit a nearly spherical morphology, which is actually a composite structure; the average particle size increased slightly from ~20 to ~30 nm, indicating that the γ′/γ″-coprecipitates were still stable after aging at 700°C for 100 h. When the aging time was extended to 1000 h, the γ′/γ″-coprecipitates decomposed and the γ″ precipitates coarsened to larger disk-like shapes, whereas the γ′ precipitates remained fine and spherical (Fig. 2(b)).

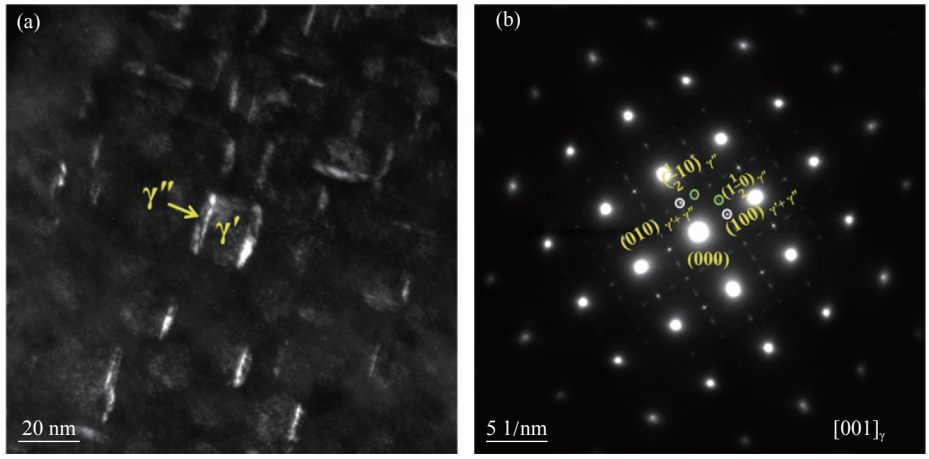

Fig. 1. Dark-field TEM morphology and diffraction pattern of the intragranular particles after solution + two-stage aging cycles in the modified Inconel 718 alloy (Al/Ti ratio ≈ 1:1): (a) dark-field TEM morphology of the γ′/γ″ coprecipitates; (b) diffraction pattern along the $[001]_\gamma$ orientation; the super lattice reflection for spherical γ′ precipitates is encircled in white, and the γ″ phase is encircled in white and green.

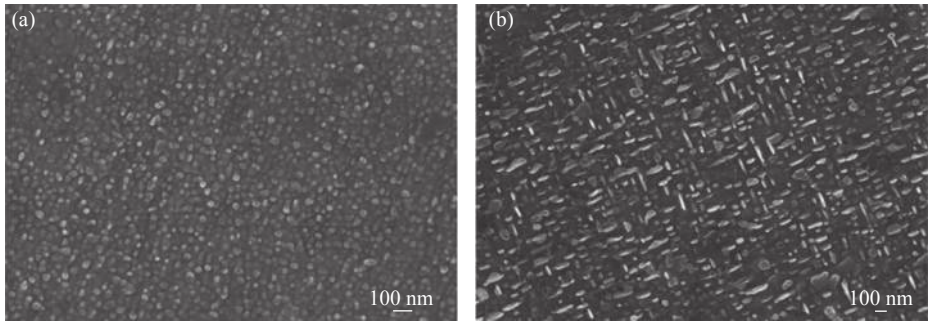

Fig. 2. SEM morphologies of the intragranular particles after aging at 700°C for different times in the modified Inconel 718 alloy (Al/Ti ratio ≈ 1:1): (a) spherical γ′/γ″ coprecipitates aged for 100 h; (b) coarsened disk-like γ″ and spherical γ′ particles aged for 1000 h.

To further verify the thermal stability of the γ′/γ″-coprecipitates, the prepared sample after the standard solution + aging treatment was aged at 800°C for 100 h; the SEM and TEM morphologies are shown in Figs. 3(a) and 3(b), and the corresponding composition of the γ′ phase indicated by arrow in Fig. 3(a) is presented in Fig. 3(c). The γ″ phase grew faster than the γ′ phase at 800°C; therefore, the γ′/γ″ coprecipitates decomposed rapidly into two independent phases of γ″ and γ′, respectively. The γ″ phase grew large, whereas the γ′ phase remained tiny. The average particle size of the γ″ phase increased from 20 to 200–500 nm, whereas the γ′ phase remained fine and spherical.

Interfaces play an essential role in the thermal stability of precipitates for the modified Inconel 718 alloys [29]. Previous studies [28,30–31] confirmed that the atoms at both sides of the interfaces of γ″/γ′, γ′/γ, and γ″/γ are perfectly matched to each other; therefore, the interfaces are completely coherent, which effectively hinders the diffusion of Al, Ti, and Nb atoms at the interfaces. According to the formation mechanism of precipitates [32], the growth of wide faces of plate-like precipitates is inhibited at fully coherent or semi-coherent interfaces. Therefore, the coarsening of the γ″ phase in the ver-

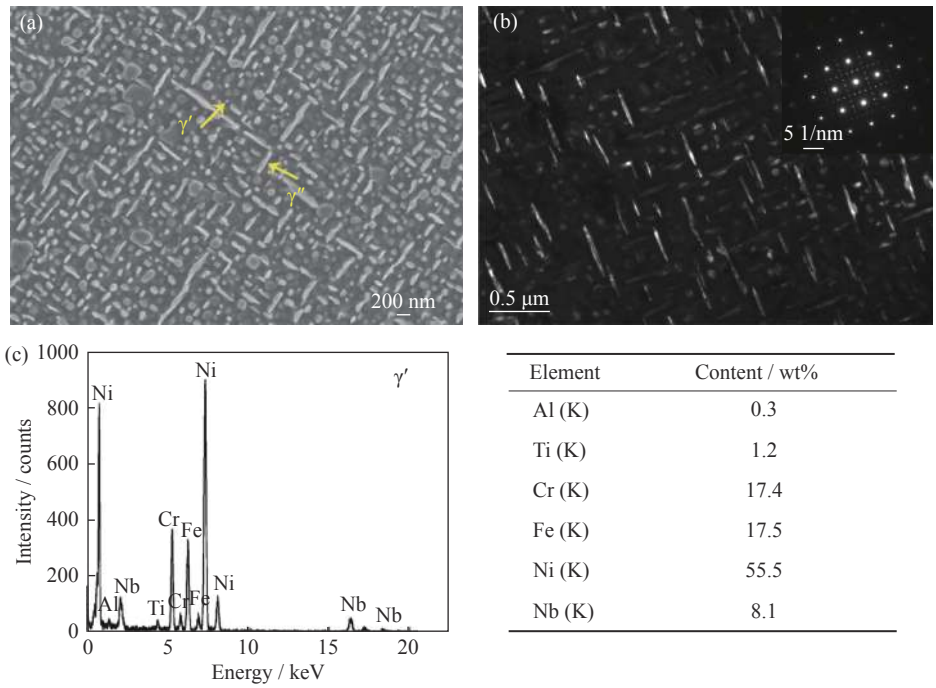

Element	Content / wt%
Al (K)	0.3
Ti (K)	1.2
Cr (K)	17.4
Fe (K)	17.5
Ni (K)	55.5
Nb (K)	8.1

Fig. 3. SEM (a) and dark-field TEM (b) morphologies of the intragranular particles in the modified Inconel 718 alloy (Al/Ti ratio ≈ 1:1) after aging at 800°C for 100 h; (c) the EDS result of the γ′ phase in (a).

tical direction of the disk plane becomes difficult, whereas the γ″ phase can grow to a larger size along the parallel direction of the disk plane. In the γ′/γ″ coprecipitate composite structure, the γ″ phase still grows along the parallel direction of the disk plane. Because of the different coarsening rates of the γ″ and γ′ phases, the coherency of the γ″/γ′ interface is destroyed during the long-term aging process; thus, the γ′/γ″ coprecipitate composite structure disappears. As a result, the γ′/γ″ composite structure remains unstable at temperatures greater than 650°C.

3.1.2. Isolated γ′ phase (Al/Ti ratio ≈ 2:1, wt%)

After the standard solution + two-stage aging cycles, fine spherical precipitates were observed in the modified alloy with an Al/Ti ratio of 2:1 (wt%), as shown in Fig. 4(a). The average particle size of the precipitates is approximately 10 nm. The selected-area diffraction pattern ($[001]_\gamma$, Fig. 4(b)) confirms that only the $L1_2$-γ′ superlattice diffraction pattern is observed, whereas the reflections corresponding to the γ″ phase are missing, indicating that the γ″ phase is not present in this modified alloy. The specimens were aged at 700°C for 100 to 1000 h to investigate the thermal stability of the γ′ phase and to detect the possible precipitation of the γ″ phase; the corresponding SEM morphologies are shown in Fig. 5. During the aging process from 100 to 1000 h, the intragranu-

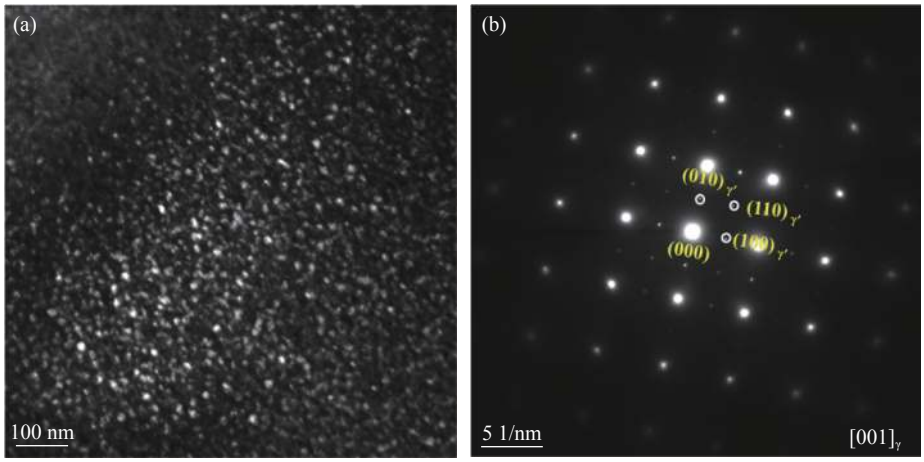

Fig. 4. Dark-field TEM morphology and diffraction pattern of the intragranular particles after solution + two-stage aging cycles in the modified Inconel 718 alloy (Al/Ti ratio ≈ 2:1): (a) dark-field TEM morphology of the isolated spherical γ′ particles; (b) the corresponding diffraction pattern along the $[001]_\gamma$ direction; the super lattice reflection for spherical γ′ precipitates is encircled in white.

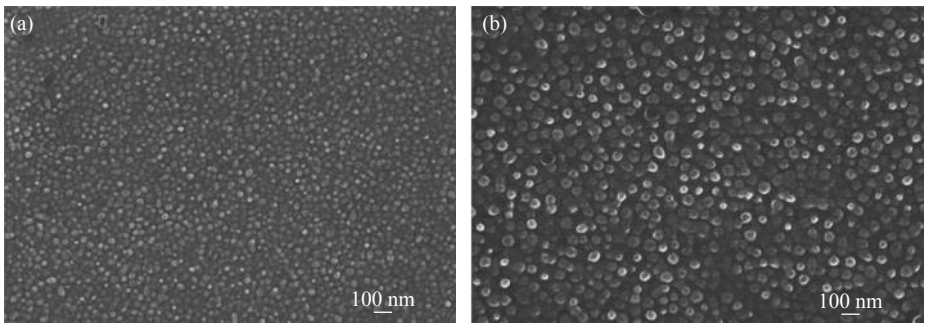

Fig. 5. SEM morphologies of the intragranular spherical γ′ particles after aging at 700°C for (a) 100 h and (b) 1000 h in the modified Inconel 718 alloy (Al/Ti ratio ≈ 2:1).

lar particles remained spherical, whereas the average size increases from ~30 nm for 100 h (Fig. 5(a)) to ~50 nm for 1000 h (Fig. 5(b)). Therefore, the γ″ phase disappeared when the Al/Ti ratio was changed to 2:1, and the results show that the isolated spherical γ′ phase exhibits improved thermal stability at 700°C compared with the γ′/γ″ coprecipitates.

To further evaluate the thermal stability of the isolated γ′ phase for temperatures higher than 700°C, the samples after standard solution + aging treatment were annealed at 800°C for 100 to 500 h, during which the γ′ phase retained its spherical shape and its average particle size increased from ~60 nm at 100 h (Fig. 6(a)) to ~100 nm at 500 h (Fig. 6(b)). In comparison with aforementioned aging results at 700°C, the isolated γ′ phase coarsened more rapidly at this case. According to the EDS analysis presented in Fig. 6(c), the γ′ phase in this modified alloy with an Al/Ti ratio of 2:1 (wt%) is rich in Al (4.7, wt%), Ti (3.3, wt%), and Nb (10.6, wt%) compared with the alloy with a modified Al/Ti ratio of 1:1. Previous studies have confirmed that Nb has a certain solubility in the γ′ phase [18,33]; thus, increasing the proportion of the γ′ phase in the alloy leads to an increase in the total content of Nb in the γ′ phase, thereby reducing the amount of Nb in the matrix, and preventing the formation of the γ″ phase. Nb reduces the coarsening rate of the γ′ phase because of its nature of sluggish diffusion kinetics as well as its high melting point. Therefore, the dissolution of Nb in the γ′ phase and the disappearance of the γ″ phase impart the isolated spherical γ′ phase with improved thermal stability at enhanced temperatures.

3.1.3. γ′/γ″/γ′ composite structure (Al/Ti ratio ≈ 3:1, wt%)

The Al/Ti ratio was increased to 3:1 (wt%), and the samples after the standard solution + aging treatment were aged at 700°C from 100 to 1000 h; the corresponding SEM morphologies of the precipitates are shown in Fig. 7(a)

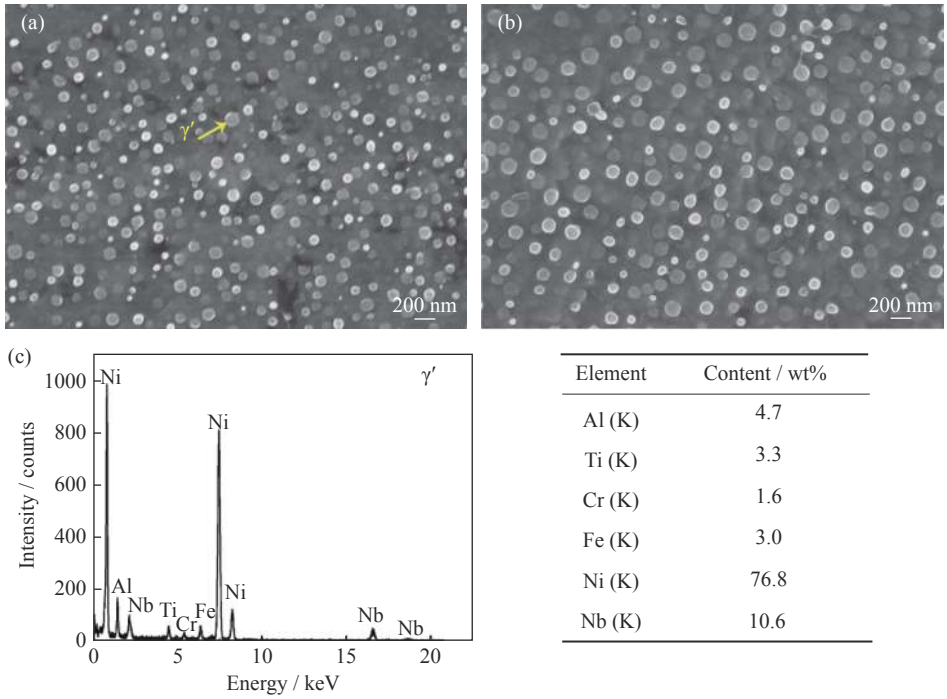

Element	Content / wt%
Al (K)	4.7
Ti (K)	3.3
Cr (K)	1.6
Fe (K)	3.0
Ni (K)	76.8
Nb (K)	10.6

Fig. 6. SEM morphologies of the intragranular γ′ particles after aging at 800°C for (a) 100 h and (b) 500 h in the modified Inconel 718 alloy (Al/Ti ratio ≈ 2:1); (c) the EDS result of the γ′ phase in (a).

(100 h) and Fig. 7(b) (1000 h), respectively. The intragranular strengthening particles remain spherical, similar to the isolated γ′ in the modified alloy with an Al/Ti ratio of 2:1 (wt%), and the particle size reaches ~60 nm after 1000 h. The dark-field TEM image of the spherical precipitates is presented in Fig. 8, where a particle is defined as an ellipsoidal phase embellished with a disc-shaped core in the middle. The selected-area electron diffraction (SAED) pattern along the $[001]_\gamma$ direction indicates the superlattice reflections of both $L1_2$-γ′ and $D0_{22}$-γ″; thus, this composite precipitate is determined as γ′/γ″/γ′, where a thin γ″ phase exists on ellipsoidal γ′ particles. In comparison with the modified Inconel 718 alloy with an Al/Ti ratio of 1:1 (wt%), the composite γ′/γ″/γ′ precipitates in this alloy appear to have smaller sizes after aging at 700°C for 1000 h (Fig. 7(b)); thus, the γ′/γ″/γ′ composite structure exhibits improved thermal stability compared with the γ′/γ″ composite structure aged at 700°C.

The samples after standard solution + aging treatment are subjected to aging at 800°C from 100 to 500 h, and the corresponding SEM morphologies of the intragranular phase are shown in Fig. 9, where the composite γ′/γ″/γ′ precipitates remain spherical after the aging treatment at 800°C. Furthermore, the γ′/γ″/γ′ composite precipitate only increases in particle size; no decomposition occurs during the aging process. Under the same aging conditions at 800°C, the amount of spherical γ′ precipitates increases when the Al/Ti ratio is increased from 2:1 to 3:1; this effect is induced by the increase in the Al concentration [32]. Otherwise, the composite γ′/γ″/γ′ precipitates showed faster coarsening behavior than the isolated γ′ phase at 800°C.

The composite structure and matching interfaces between the precipitates are believed to play an essential role in the thermal stability. In Inconel 718 alloy, Al atoms are segregated at the γ′/γ″ interface [34–35] and the segregation of Al atoms suppresses the diffusion of Nb from the γ′ to the γ″ phase, and inhibits Al from the γ″ to the γ′ phase; thus, the precipitates retain their stable composite structure [36]. Meanwhile, more Nb dissolves into the γ′ phase because of the increase in Al concentration, and the diffusion of Nb in the γ′ phase is restricted by the matching interface between γ″ and γ′; therefore, the γ″ growth is limited by adjacent γ′ and the coarsening process of the γ′/γ″/γ′ composite precipitate is mainly controlled by the γ′ phase. In addition, the coherency relationship between γ″/γ, γ′/γ, and γ″/γ′ also promotes the

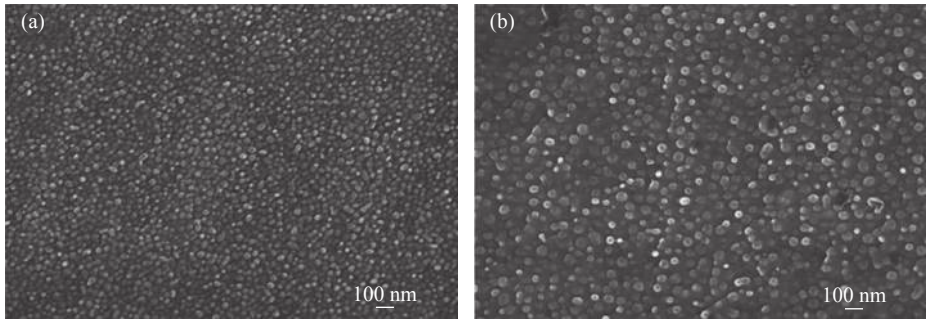

Fig. 7. SEM morphologies of the intragranular spherical composite precipitates (γ′/γ″/γ′) after aging at 700°C for (a) 100 h and (b) 1000 h in the modified Inconel 718 alloy (Al/Ti ratio ≈ 3:1).

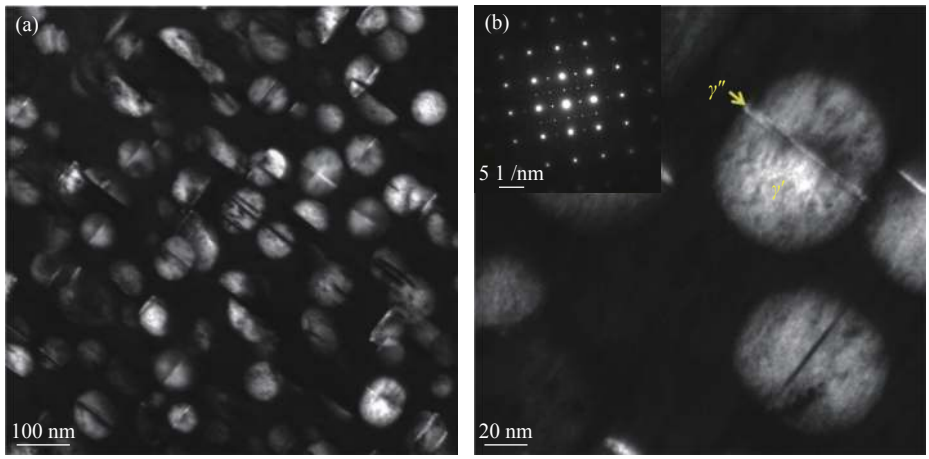

Fig. 8. Dark-field TEM morphology and the selected-area electron diffraction pattern after aging at 700°C for 1000 h in the modified Inconel 718 alloy (Al/Ti ratio ≈ 3:1): (a) dark-field TEM morphology of the spherical composite precipitates (γ′/γ″/γ′); (b) the SAED pattern along the $[001]_\gamma$ direction; the super lattice reflection for both γ′ and γ″.

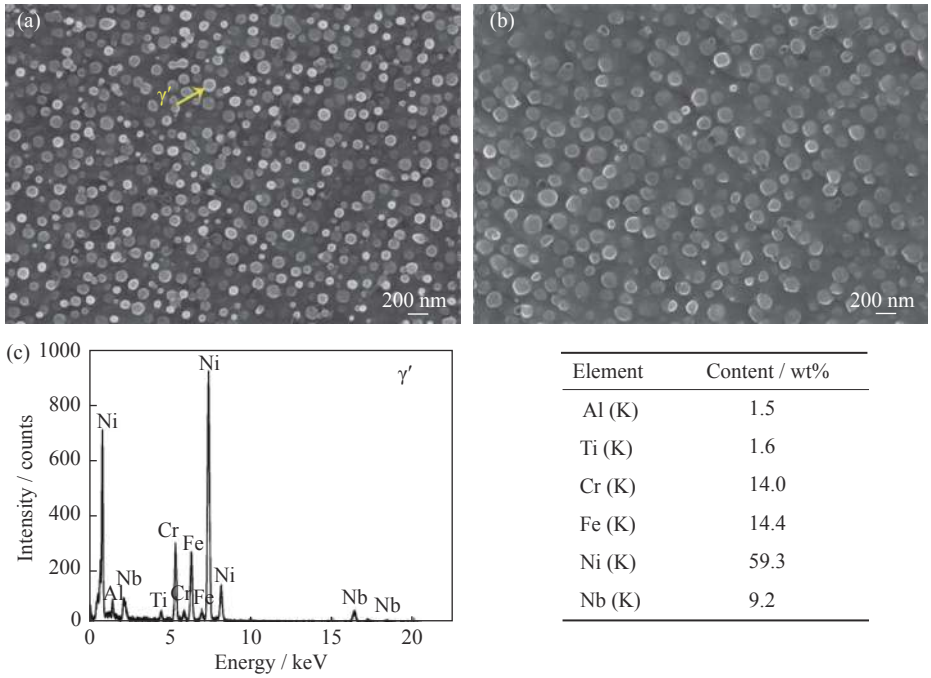

Element	Content / wt%
Al (K)	1.5
Ti (K)	1.6
Cr (K)	14.0
Fe (K)	14.4
Ni (K)	59.3
Nb (K)	9.2

Fig. 9. SEM morphologies of the intragranular spherical composite precipitates (γ′/γ″/γ′) after aging at 800°C for (a) 100 h and (b) 500 h in the modified Inconel 718 alloy (Al/Ti ratio ≈ 3:1); (c) the EDS result of the γ′ phase.

stability of the γ′/γ″/γ′ precipitates. This stability, combined with the aforementioned reasons, is responsible for the composite precipitate (γ′/γ″/γ′) exhibiting greater thermal stability than the coprecipitate (γ′/γ″).

3.2. Role of Al/Ti ratios on precipitation behavior

Al is a γ′-forming element and can increase the γ′ solvus and fraction [37]; thus, the Al concentration has a critical influence on the precipitation behavior of the γ′ and γ″ phases in Inconel 718 alloy [38]. With an increase of the Al content, the γ″ and γ′ phases changed into isolated or composite precipitates with improved structural stability compared with that of conventional Inconel 718 alloy at elevated temperatures. The experimental results demonstrate that a higher Al/Ti ratio results in a larger amount of fine, spherical precipitates. Engel–Brewer theory proposed that the number of s and p valence electrons determined the crystal structure of the compound [39]. Analysis of the ratio between the concentration of electrons and atoms indicates that the precipitation of the $L1_2$-γ′ phase can occur in a certain range of electron/atom (e/a) ratios and that the most effective ratio is 3.0. Because the e/a ratio of Al is 3.0, Al promotes the formation of the γ′ phase [40]. Simultaneously, the addition of Al reduces the lattice parameters of the matrix and the metastable phase, resulting in a decrease in interfacial energy. Therefore, increasing Al addition can convert the Inconel 718 alloy into a predominantly γ′ strengthening alloy, with improved thermal structural stability.

When Al/Ti ratio ≈ 1:1, the γ′ generates first, forming an Nb-rich region nearby so that the γ″ nucleates in the same direction on both sides of γ′ particle and finally forms γ′/γ″ coprecipitates. When Al/Ti ratio ≈ 2:1, the increase of the Al content induces the formation of more γ′ phase. Because the Al atoms in the γ′ lattice can be replaced by Ti and Nb, more Nb is dissolved in the γ′ phase (Table 2), resulting in a decrease in the Nb content in the matrix to reduce γ″ formation; in this case, only isolated γ′ phase forms after aging because of the increased Al/Ti ratio of 2:1. At this point, the Al and Nb contents reach a relative equilibrium state, enabling the γ′ phase to exist without the formation of the γ″ phase. When Al/Ti ratio ≈ 3:1, the excessive Al content reduces the Nb concentration in the γ′ phase to some extent, which leads to a portion of the Nb in the forming γ″-phase precipitates; thus, another composite γ′/γ″/γ′ structure is formed. Here we propose a hypothesis for the γ″ formation mechanism. At the beginning of the aging stage, the fresh spherical γ′ phase is rich in more Nb; as a result, the lattice distortion and internal energy of the γ′ phase increases because of the large atomic size and number of Nb atoms. To stabilize the γ′ phase, some Nb atoms dissolve into the matrix, which reduces the lattice distortion of the γ′ phase. The increase of the Nb content in the matrix promotes the formation of some γ″ phase. However,

Table 2. Chemical compositions of the formed γ′ phase in the modified Inconel 718 alloys with different Al/Ti ratios after the samples were aged at 800°C for 100 h wt%

Specimen	Al	Ti	Nb
Al/Ti ratio ≈ 1:1	0.3	1.2	8.2
Al/Ti ratio ≈ 2:1	4.7	3.3	10.6
Al/Ti ratio ≈ 3:1	1.5	1.6	9.2

the formation mechanism of this structure is still not clear and further research is needed. Nonetheless, it is speculated that changing the Al/Ti ratio can lead to the formation of an isolated γ′ strengthening phase but its formation only occurs within a certain ratio range. A comparison of the composition with that of ATI 718Plus [41] suggests that the transition of the strengthening phase depends on the Al/Ti ratio, especially the Al content.

The aforementioned results reveal that the thermal stability of precipitates depends on the morphology and elemental compositions. Because the γ′/γ″ interface is coherent, the γ′/γ″ coprecipitates exhibit good thermal stability within a short aging time. With the extension of the aging time, the coherency the crystallographic relationship at the interface is destroyed because of the different coarsening rates of the γ′ and γ″ phases, and the γ′/γ″ composite structure decomposes. The aging results demonstrate that the γ′/γ″/γ′ composite precipitates are more stable than the γ′/γ″ composite precipitates and that the coarsening of the γ′/γ″/γ′ composite structure is mainly controlled by the γ′ phase. On the one hand, the γ′ phase in the γ′/γ″/γ′ composite structure contains more Nb (Table 2), which inhibits the growth of the γ″ phase. On the other hand, the Al atoms enriched at the γ′/γ″ interfaces hinder the atomic diffusion of Nb, which restrains the growth of the γ″ phase.

3.3. Coarsening behavior of the isolated γ′ and γ′/γ″/γ′

Previous studies [42–45] in the traditional Inconel 718 alloy have shown that the coarsening of the γ” and γ' phases is controlled by atomic diffusion, following the Lifshitz–Slyozov–Wagner (LSW) theory [7]. Similarly, the coarsening of isolated spherical γ′ phase and composite structure precipitates (γ′/γ″/γ′) still follows the LSW theory, as shown in Fig. 10; that is, a relationship exists between the precipitate phase size (d_t^3, where d_t is the average particle diameter after aging for time t) and the aging time (t). As the aging temperature increases, the coarsening rate of the precipitate increases rapidly (Figs. 10(a) and 10(b)). At the same aging temperature, the coarsening rate of the isolated γ′ phase is lower than that of the composite precipitates (γ′/γ″/γ′) (Figs. 10(c) and 10(d)) because the isolated γ′ phase has a higher Nb content than the γ′ phase in the γ′/γ″/γ′ composite precipitates (Table 2); the Nb content can effectively lower the γ′ coarsening rate [46]. In addition, increasing the Al content promotes the formation and growth of the γ′ phase; thus, the coarsening rate of the isolated γ′ is lower than the γ′/γ″/γ′ composite precipitates with Al/Ti ratios increasing from 2:1 to 3:1.

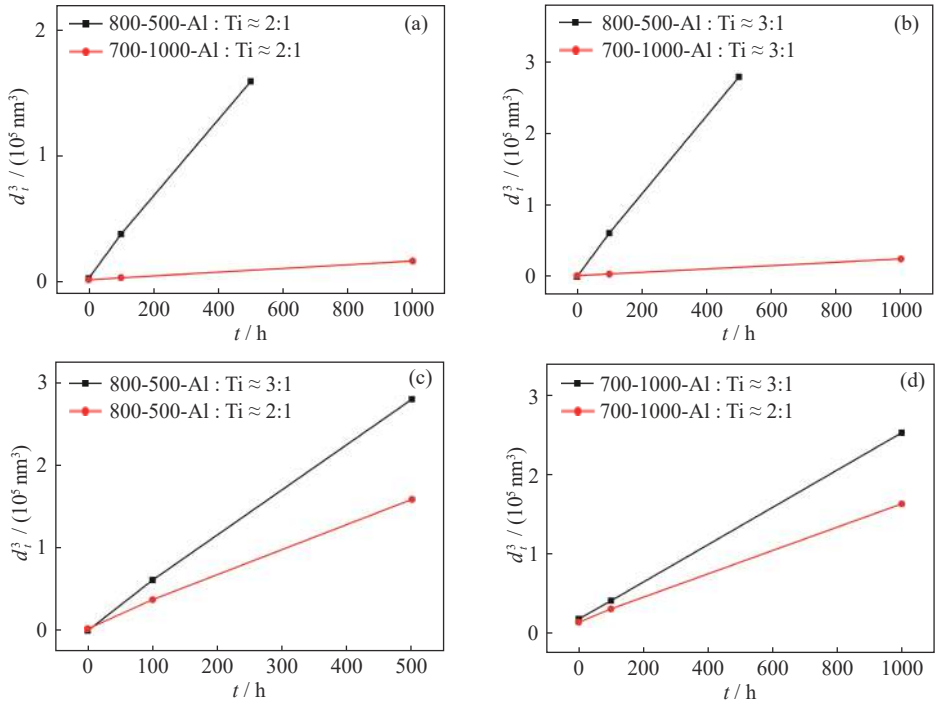

Fig. 10. Coarsening curves of the γ′ and γ′/γ″/γ′ precipitates of the modified Inconel 718 alloy with different Al/Ti ratios: (a) aging at 800°C for 500 h and aging at 700°C for 1000 h (Al/Ti ratio ≈ 2:1); (b) aging at 800°C for 500 h and aging at 700°C for 1000 h (Al/Ti ratio ≈ 3:1); (c) aging at 800°C for 500 h (Al/Ti ratio ≈ 3:1 and 2:1); (d) aging at 700°C for 1000 h (Al/Ti ratio ≈ 3:1 and 2:1).

4. Conclusions

The precipitation behavior and thermal stability of precipitates with various morphologies in modified Inconel 718 alloy were investigated by aging at 700–800°C for 100–1000 h. The following conclusions have been reached.

(1) Three types of precipitates configuration are formed through modification of the Al/Ti ratios: γ′/γ″ coprecipitates, isolated spherical γ′, and γ′/γ″/γ′ composite precipitates, which are obtained in modified Inconel 718 alloy with Al/Ti ratios of 1:1, 2:1, and 3:1 (wt%), respectively.

(2) The isolated γ′ and γ′/γ″/γ′ composite precipitates exhibit better thermal stability at temperature as high as 800°C. The isolated γ′ phase exhibits a lower coarsening rate compared with the γ′/γ″/γ′ composite particles because the isolated γ′ phase is rich in Al, Ti, and Nb. The γ′/γ″ coprecipitates coarsen and decompose quickly during thermal aging at temperatures greater than 700°C because of the lower stability resulting from the larger number of γ″ particles.

Acknowledgements

This work was financially supported by the National Natural Science Foundation of China (Nos. 51474156 and U1660201) and the National High Technology Research and Development Program of China (No. 2015AA042504).

References

[1] Y.C. Liu, Q.Y. Guo, C. Li, Y.P. Mei, X.S. Zhou, Y. Huang, and H.J. Li, Recent progress on evolution of precipitates in Inconel 718 superalloy, *Acta Metall. Sin.*, 52(2016), No. 10, p. 1259.

[2] X. Zhang, H.W. Li, M. Zhan, Z.B. Zheng, J. Gao, and G.D. Shao, Electron force-induced dislocations annihilation and regeneration of a superalloy through electrical *in-situ* transmission electron microscopy observations, *J. Mater. Sci. Technol.*, 36(2020), p. 79.

[3] H.J. Zhang, C. Li, Y.C. Liu, Q.Y. Guo, and H.J. Li, Precipitation behavior during high-temperature isothermal compressive deformation of Inconel 718 alloy, *Mater. Sci. Eng. A*, 677(2016), p. 515.

[4] H.J. Zhang, C. Li, Y.C. Liu, Q.Y. Guo, Y. Huang, H.J. Li, and J.X. Yu, Effect of hot deformation on γ″and δ phase precipitation of Inconel 718 alloy during deformation & isothermal treatment, *J. Alloys Compd.*, 716(2017), p. 65.

[5] H.J. Zhang, C. Li, Q.Y. Guo, Z.Q. Ma, Y. Huang, H.J. Li, and Y.C. Liu, Delta precipitation in wrought Inconel 718 alloy; the role of dynamic recrystallization, *Mater. Charact.*, 133(2017), p. 138.

[6] K. Chen, S.Y. Rui, F. Wang, J.X. Dong, and Z.H. Yao, Microstructure and homogenization process of as-cast GH4169D alloy for novel turbine disk, *Int. J. Miner. Metall. Mater.*, 26(2019), No. 7, p. 889.

[7] Y. Han, P. Deb, and M.C. Chaturvedi, Coarsening behaviour of γ″-and γ'-particles in Inconel alloy 718, *Met. Sci.*, 16(1982), No. 12, p. 555.

[8] K. Sano, N. Oono, S. Ukai, S. Hayashi, T. Inoue, S. Yamashita, and T. Yoshitake, γ″-Ni3Nb precipitate in Fe–Ni base alloy, *J. Nucl. Mater.*, 442(2013), No. 1-3, p. 389.

[9] C.K.L. Davies, P. Nash, and P.N. Steven, The effect of volume fraction of precipitate on Ostwald ripening, *Acta Metall.*, 28(1980), No. 2, p. 179.

[10] J. Wu, Y.C. Liu, C. Li, Y.T. Wu, X.C. Xia, and H.J. Li, Recent progress of microstructure evolution and performance of multiphase Ni_3Al-based intermetallic alloy with high Fe and Cr contents, *Acta Metall. Sin.*, 56(2020), No. 1, p. 21.

[11] J.P. Collier, S.H. Wong, J.K. Tien, and J.C. Phillips, The effect of varying AI, Ti, and Nb content on the phase stability of INCONEL 718, *Metall. Trans. A*, 19(1988), No. 7, p. 1657.

[12] M. Sundararaman, P. Mukhopadhyay, and S. Banerjee, Precipitation and room temperature deformation behavior of Inconel 718, [in] *Proceedings of Third International Symposium on Superalloys 718, 625, 706 and Various Derivatives*, Pittsburgh, 1994, p. 419.

[13] E.C. Guo and F.Q. Xu, Superalloy 718—Metallurgy and Applications, [in] *Proceedings of the International Symposium on the Metallurgy and Applications of Superalloy 718*, Pittsburgh, 1989, p. 567.

[14] J.X. Dong, X.S. Xie, and S.H. Zhang, Enhancements of thermal structure stability in Ni-base superalloy, *Scr. Metall. Mater.*, 28(1993), No. 12, p. 1477.

[15] Y.L. Shao, J. Xu, H. Wang, Y.W. Zhang, J. Jia, J.T. Liu, H.L. Huang, M. Zhang, Z.C. Wang, H.F. Zhang, and B.F. Hu, Effect of Ti and Al on microstructure and partitioning behavior of alloying elements in Ni-based powder metallurgy superalloys, *Int. J. Miner. Metall. Mater.*, 26(2019), No. 4, p. 500.

[16] D. Zhao and P.K. Chaudhury, Effect of starting grain size on as-deformed microstructure in high temperature deformation of alloy 718, [in] *Proceedings of Third International Symposium on Superalloys 718, 625, 706 and Various Derivatives*, Pittsburgh, 1994, p. 303.

[17] X.S. Xie, G.L. Wang, J.X. Dong, C.M. Xu, W.D. Cao, and R.L. Kennedy, Structure stability study on a newly developed nickel-base superalloy—Allvac® 718Plus™, [in] *Proceedings of the Sixth International Symposium on Superalloys 718, 625, 706 and Derivatives*, Pittsburgh, 2005, p. 179.

[18] S.H. Fu, J.X. Dong, M.C. Zhang, and X.S. Xie, Alloy design and development of INCONEL718 type alloy, *Mater. Sci. Eng. A*, 499(2009), No. 1-2, p. 215.

[19] J.P. Collier, A.O. Selius, and J.K. Tien, On developing a microstructurally and thermally stable iron–nickel base superalloy, [in] *Superalloys 1988*, Warrendale, 1988, p. 43.

[20] R.B. Bhavsar, A. Collins, and S. Silverman, Use of alloy 718 and 725 in oil and gas industry, [in] *Proceedings of the Fifth International Symposium on Superalloys 718, 625, 706 and Various Derivatives*, Pittsburgh, 2001, p. 47.

[21] J.F. Radavich and D.J. Meyers, Thermomechanical processing of P/M alloy 718, [in] *Superalloys 1984*, Pittsburgh, 1984, p. 347.

[22] J.F. Radavich and W.H. Couts, Factors affecting delta phase precipitation and growth at hot work temperatures for direct aged IN718, [in] *Superalloys 1984*, Pittsburgh, 1984, p. 497.

[23] S. Antonov, M. Detrois, R.C. Helmink, and S. Tin, Precipitate phase stability and compositional dependence on alloying additions in γ–γ'–δ–η Ni-base superalloys, *J. Alloys Compd.*, 626(2015), p. 76.

[24] N. Paton, T. Cabral, K. Bowen, and T. Tom, Spraycast-X IN718 processing benefits, [in] *Proceedings of the Fourth International Symposium on Superalloys 718, 625, 706 and Various Derivatives*, Warrendale, 1997, p. 1.

[25] R. Cozar and A. Pineau, Morphology of γ' and γ″ precipitates and thermal stability of inconel 718 type alloys, *Metall. Trans.*, 4(1973), p. 47.

[26] S.T. Wlodek and R.D. Field, The effect of long time exposure on alloy 718, [in] *Proceedings of Third International Symposium on Superalloys 718, 625, 706 and Various Derivatives*, Pittsburgh, 1994, p. 659.

[27] C. Ruiz, A. Obabueki, and K. Gillespie, Evaluation of the microstructure and mechanical properties of delta processed alloy 718, [in] *Superalloy 1992*, Warrendale, 1992, p. 33.
[28] J. He, G. Han, S. Fukuyama, and K. Kokogawa, Interfaces in a modified Inconel 718 with compact precipitates, *Acta Mater.*, 46(1998), No. 1, p. 215.
[29] A.J. Ardell, Precipitation hardening, *Metall. Trans. A*, 16(1985), p. 2131.
[30] M.K. Miller, S.S. Babu, and M.G. Burke, Comparison of the phase compositions in alloy 718 measured by atom probe tomography and predicted by thermodynamic calculations, *Mater. Sci. Eng. A*, 327(2002), No. 1, p. 84.
[31] P.J. Phillips, D. Mcallister, Y.P. Gao, D.C. Lv, R.E.A. Williams, B. Peterson, Y.Z. Wang, and M.J. Mills, Nano γ'/γ″ composite precipitates in Alloy 718, *Appl. Phys. Lett.*, 100(2012), art. No. 211913.
[32] Q.Y. Guo, Y.M. Li, B. Chen, R. Ding, L.M. Yu, and Y.C. Liu. Effect of high-temperature ageing on microstructure and creep properties of S31042 heat-resistant steel, *Acta Metall. Sin.,* 2020. https://doi.org/10.11900/0412.1961.2020.00109.
[33] A.J. Detor, R. DiDomizio, R. Sharghi–Moshtaghin, N. Zhou, R.P. Shi, Y.Z. Wang, D.P. McAllister, and M.J. Mills, Enabling large superalloy parts using compact coprecipitation of γ' and γ'', *Metall. Mater. Trans. A*, 49(2018), No. 3, p. 708.
[34] K. Kulawik, P.A. Buffat, A. Kruk, A.M. Wusatowska–Sarnek, and A. Czyrska–Filemonowicz, Imaging and characterization of γ' and γ″ nanoparticles in Inconel 718 by EDX elemental mapping and FIB–SEM tomography, *Mater. Charact.*, 100(2015), p. 74.
[35] N. Zhou, C. Shen, M.J. Mills, J. Li, and Y.Z. Wang, Modeling displacive–diffusional coupled dislocation shearing of γ' precipitates in Ni-base superalloys, *Acta Mater.*, 59(2011), No. 9, p. 3484.
[36] W.T. Geng, D.H. Ping, Y.F. Gu, C.Y. Cui, and H. Harada, Stability of nanoscale co-precipitates in a superalloy: A combined first-principles and atom probe tomography study, *Phys. Rev. B*, 76(2007), art. No. 224102.
[37] X.S. Xie, S.H. Fu, S.Q. Zhao, and J.X. Dong, The precipitation strengthening effect of Nb, Ti and Al in cast/wrought Ni-base superalloys, *Mater. Sci. Forum*, 638-642(2010), p. 2363.
[38] A.K. Jena and M.C. Chaturvedi, The role of alloying elements in the design of nickel-base superalloys, *J. Mater. Sci.*, 19(1984), No. 10, p. 3121.
[39] W. Hume–Rothery, The Engel–Brewer theories of metals and alloys, *Prog. Mater. Sci.*, 13(1968), p. 229.
[40] J. Wu, C. Li, Y.C. Liu, Y.T. Wu, Q.Y. Guo, H.J. Li, and H.P. Wang, Effect of annealing treatment on microstructure evolution and creep behavior of a multiphase Ni_3Al-based superalloy, *Mater. Sci. Eng. A*, 743(2019), p. 623.
[41] M.Q. Wang, J.H. Du, Q. Deng, Z.L. Tian, and J. Zhu, Effect of the precipitation of the η-$Ni_3Al_{0.5}Nb_{0.5}$ phase on the microstructure and mechanical properties of ATI 718Plus, *J. Alloys Compd.*, 701(2017), p. 635.
[42] M. Sundararaman, P. Mukhopadhyay, and S. Banerjee, Some aspects of the precipitation of metastable intermetallic phases in Inconel 718, *Metall. Trans. A*, 23(1992), No. 7, p. 2015.
[43] M. Sundararaman and P. Mukhopadhyay, Overlapping of γ' precipitate variants in Inconel 718, *Mater. Charact.*, 31(1993), No. 4, p. 191.
[44] C. Slama, C. Servant, and G. Cizeron, Aging of the Inconel 718 alloy between 500 and 750°C, *J. Mater. Res.*, 12(1997), No. 9, p. 2298.
[45] Y.C. Liu, H.J. Zhang, Q.Y. Guo, X.S. Zhou, Z.Q. Ma, Y. Huang, and H.J. Li, Microstructure evolution of Inconel 718 superalloy during hot working and its recent development tendency, *Acta Metall. Sin.*, 54(2018), No. 11, p. 1653.
[46] Y.T. Wu, Y.C. Liu, C. Li, X.C. Xia, J. Wu, and H.J. Li, Coarsening behavior of γ' precipitates in the γ' + γ area of a Ni_3Al-based alloy, *J. Alloys Compd.*, 771(2019), p. 526.